Published in final edited form as:
Dev Biol. 2005 December 15; 288(2): 334–347. doi:10.1016/j.ydbio.2005.08.018.

BMP7 inhibits branching morphogenesis in the prostate gland and interferes with Notch signaling

Irina B. Grishina[a,*], **Sung Yup Kim**[a], **Christopher Ferrara**[a], **Helen P. Makarenkova**[b], and **Paul D. Walden**[a]

a*Department of Urology, New York University School of Medicine, VAMC, 423 East 23rd Street, 18064-South, New York, NY 10010, USA*

b*The Neuroscience Institute, 10640 John Jay Hopkins Drive, San Diego, CA 92121, USA*

Abstract

The mouse prostate gland develops by branching morphogenesis from the urogenital epithelium and mesenchyme. Androgens and developmental factors, including FGF10 and SHH, promote prostate growth, while BMP4 signaling from the mesenchyme has been shown to suppresses prostate branching. Here, we show that Bone Morphogenetic Protein 7 (BMP7) restricts branching of the prostate epithelium. *BMP7* is expressed in the periurethral urogenital mesenchyme prior to formation of the prostate buds and, subsequently, in the prostate epithelium. We show that $BMP7^{lacZ/lacZ}$ null prostates show a two-fold increase in prostate branching, while recombinant BMP7 inhibits prostate morphogenesis in organ culture in a concentration-dependent manner. We further explore the mechanisms by which the developmental signals may be interpreted in the urogenital epithelium to regulate branching morphogenesis. We show that Notch1 activity is associated with the formation of the prostate buds, and that Notch1 signaling is derepressed in *BMP7* null urogenital epithelium. Based on our studies, we propose a model that BMP7 inhibits branching morphogenesis in the prostate and limits the number of domains with high Notch1/Hes1 activity.

Keywords

BMP7; pSmad1; Notch1; Hes1; Prostate; Branching morphogenesis; Urogenital sinus; Epithelium; Mesenchyme

Introduction

The prostate is a sex-accessory exosecretory gland in mammalian males. The prostate retains the ability to support cell replication, differentiation and morphogenesis throughout adult life, and is prone to benign and malignant tumors (for review see Abate-Shen and Shen, 2000; Marker et al., 2003). The prostate develops by branching morphogenesis from the epithelium and mesenchyme of the urogenital sinus, an enlarged portion of the urethra beneath the bladder. Prostate morphogenesis begins around embryonic day 16 (E16) in mouse when the primary epithelial buds originate from the urogenital sinus epithelium at particular dorso-ventral and anterior-posterior positions (Abate-Shen and Shen, 2000; Marker et al., 2003; and this report). At E16-E19, prostate buds extend through the urogenital sinus mesenchyme by proliferation of the ductal epithelium. Postnatally, prostate lobes grow in size, canalize and undergo lobe-specific branching. The adult prostate in mouse and human is composed of branched ducts, made of stratified epithelium, separated by the basal lamina from the fibroblast stroma and

*Corresponding author. Fax: +1 212 951 5424. *E-mail address:* irina.grishina@med.nyu.edu (I.B. Grishina).

smooth muscle (for review see Abate-Shen and Shen, 2000; Marker et al., 2003). There is some evidence pointing to the relationship between the cell fate choice and morphogenesis in the prostate. The luminal layer of the epithelium in the adult prostate contains mostly androgen-dependent secretory cells (Economides and Capecchi, 2003; Marker et al., 2003). The basal epithelial layer may contain epithelial progenitors at various stages of differentiation (Robinson et al., 1998; Wang et al., 2001; Tsujimura et al., 2002). Interestingly, cell proliferation in the prostate epithelium is concentrated to the distal tips, while the proximal areas of the ducts have been suggested to contain neuroendocrine androgen-independent cells, which may contribute to neuroepithelial prostate cancers (Abate-Shen and Shen, 2000; Foster et al., 2002; Hu et al., 2002; Marker et al., 2003).

Branching morphogenesis and differentiation of the mouse prostate depends on the signaling between the urogenital mesenchyme and epithelium mediated in part by androgens, Sonic hedgehog (SHH), Fibroblast Growth Factor 10 (FGF10) and Bone Morphogenetic Protein 4 (BMP4) (Berman et al., 2004; Donjacour et al., 2003; Freestone et al., 2003; Podlasek et al., 1999; Lamm et al., 2001). In *FGF10* null mice, the prostates and other sex-accessory glands are either absent or rudimentary (Donjacour et al., 2003). SHH signaling from the prostate epithelium, mediated by the Gli1,2,3 transcription factors in the prostate mesenchyme, is required for prostate growth and branching (Berman et al., 2004; Freestone et al., 2003; and our unpublished data). Conversely, haploinsufficiency for *BMP4* has been shown to increase prostate branching (Lamm et al., 2001), while the *BMP12/GDF7* is required for morphogenesis and differentiation of the seminal vesicles (Settle et al., 2001). We show that another member of the BMP family of ligands, *BMP7*, is expressed dynamically in the urogenital mesenchyme and prostate epithelium during prostate development. Here, we implemented gain and loss of function approaches to show that BMP7 signaling inhibits prostate branching.

The mechanisms by which the developmental signals are translated in the epithelium to initiate branching are not well understood. Recent studies have shown that signaling from the mesenchyme by FGF10 and BMP4 can modulate Notch1 activity in the epithelium during morphogenesis of the tooth bud and the pancreas (Hart et al., 2003; Mustonen et al., 2002; Norgaard et al., 2003). Studies of branching morphogenesis in the lung and submandibular gland (Hogan, 1999; Jaskoll et al., 2002) suggest that formation of the new epithelial bud begins with definition of a domain in the epithelium and adjacent mesenchyme that is committed to diverge from the main lobe and form a new branch. Indeed, one of the few evolutionary conserved mechanisms suggested to mediate formation of morphogenetic domains, is the Notch-Notch ligand cell fate selection/lateral inhibition pathway (Anderson et al., 1997; Artavanis-Tsakonas et al., 1999). For instance, in chick, Notch signaling has been shown to define positions and boundaries of the feather buds (Crowe et al., 1998). Notch signaling is activated by binding of the extracellular domain of the Notch receptor to its ligands, Delta-like 1 (Dll1) or Jagged1,2 (Jag1,2), themselves membrane receptors (Artavanis-Tsakonas et al., 1999; Small et al., 2001). In addition, interaction between Notch and Delta ligands is potentiated by Fringe glycosyltransferases (Artavanis-Tsakonas et al., 1999). Activation of the Notch receptor results in proteolytic cleavage and nuclear translocation of the Notch cytoplasmic domain, binding to the co-transactivator (RBPjk, Supressor of Hairless, Lag-1) and induction of downstream transcriptional repressors (*Hes, Hairy/Enhacer of Split*) (Tomita et al., 1996; Ohtsuka et al., 1999). In vertebrates, Hes1,5 functions downstream of Notch signaling to repress transcription of the proneural basic helix-loop-helix (bHLH) transcription factors, *Mash1*, *Math1* and *Ngn*. In vertebrates, Notch signaling has been implicated in proximal-distal patterning and differentiation of the epithelium during branching morphogenesis in the mouse lung (Post et al., 2000; Ito et al., 2000), gut (de Santa Barbara et al., 2003) and pancreas (Hart et al., 2003; Norgaard et al., 2003). *Math1* and *Ngn3* mark differentiation of the proximal neuroendocrine epithelium in the intestine and pancreas (Gradwohl et al., 2000; Murtaugh et al., 2003; Yang et al., 2001). During branching

morphogenesis in the lungs, domains of *Mash1* expression coincide with *Dll1* in the proximal and interbud regions of the lung epithelium (Post et al., 2000; Ito et al., 2000). *Mash1* has been also detected in part of the neuroendocrine epithelium during normal development of the prostate gland and in prostate cancers (Hu et al., 2002).

In the present study, we explored the interaction between BMP7 and Notch1 signaling during branching morphogenesis of the mouse prostate gland. We found that *BMP7* is expressed in the periurethral mesenchyme prior to prostate formation in embryogenesis, and that *BMP7* null prostates exhibit abnormally extensive branching. Conversely, recombinant BMP7 inhibited branching morphogenesis and *Hes1* expression in cultured urogenital explants. Our analysis revealed that domains of Notch1 activity are localized to the forming buds and distal prostate tips, and are complementary to BMP/pSmad1 signaling. Furthermore, areas of Notch1 activity were significantly broadened in *BMP7* null prostates where BMP/pSmad1 signaling is abolished in the urogenital epithelium. Based on our data, we propose a model thereby the Notch selection system is involved in defining the prebud epithelium, and BMP7 restricts prostate branching by limiting the number of domains with high Notch1 activity.

Materials and methods

Mouse lines, tissue collection and genotyping

Mice strains used were 129SvE $BMP7^{lacZ}$, a gift from Elizabeth Robertson (Godin et al., 1998), and Swiss Webster (Taconic, Germantown, NY). Embryonic day 1 (E1) was designated the day when the vaginal plug was first observed. The day of birth was designated P1. The sex of E14 and E15 embryos was determined by PCR with primers for the *Sry* gene (Gubbay et al., 1992). From E16 on, the sex of the embryos was determined by the characteristic positions of the sexually committed gonads. Genotyping of heterozygous $BMP7^{lacZ/+}$ animals was performed by staining a small tail biopsy for β-galactosidase activity (Godin et al., 1998). $BMP7^{lacZlacZ}$ null animals were identified by the lack of eyes and polydactyly of the hind limbs (Jena et al., 1997).

Tyramide-enhanced immunofluorescent analysis (TIF)

Urogenital samples were fixed in 4% PFA for 1 h, dehydrated and infused with paraffin overnight at 57°C, embedded into blocks at specified orientation and kept at 4°C. Sections were cut at 7 μm and dried at room temperature overnight. On the day of immunostaining, sections were baked for 1 h at 57°C, cleared in xylene and rehydrated in graded ethanols. Endogenous peroxidase activity was quenched for 10 min at room temperature with 3% hydrogen peroxide, followed by antigen retrieval performed by microwaving in Citrate Buffer for 30 min. Sections were blocked with 1% TSA kit blocking reagent (Molecular probes) for 1 h at room temperature, and incubated with primary antibodies diluted in blocking reagent at 4°C overnight. The next day, sections were rinsed in PBS 3 × 10 min, incubated with biotinylated secondary antibodies, rinsed in PBS 3 × 10 min followed with incubation with streptavidin-HRP for 1 h at room temperature, rinsed 3 × 10 min in PBS, and labeled with 546 Alexa Fluor Tyramide for 5 min, rinsed 3 × 10 min in PBS, counterstained with DAPI, rinsed and mounted with Gel/Mount (Biomeda, M01). Primary antibodies used were: phospho-Smad1 (Ser463/465) (Cell Signaling) at dilution 1:100; and cleaved Notch1 (Val1744) at dilution 1:50 (Cell Signaling). Immunofluorescent analysis for smooth muscle actin (sma) was performed using sma antibody (clone 1A4, DAKO) at 1:30 and 488 Alexa Fluor secondary antibodies.

In situ hybridization

In situ hybridization analysis was performed on paraffin sections with modifications (Knecht et al., 1995) as previously described (Parr et al., 1993) using digoxigenin-labeled antisense RNA probes for *BMP7* (0.9 kb), *Hes1* (1.4 kb), *Notch1* (4 kb), *Lunatic Fringe* (1.2 kb), *Maniac*

Fringe (1.4 kb), *Radical Fringe* (2.1 kb) and *Dll1* (0.6 kb). For *Hes1*, in situ analysis was also performed with TIF visualization of digoxigenin antibodies.

RT-PCR analysis

For RT-PCR analysis, total RNA was isolated from urogenital sinus samples by RNAgents Total RNA Isolation System (Promega) according to manufacture's protocol. Template RNA pools were pretreated with DNAse I and processed for RT-PCR using SuperScript One-Step RT-PCR kit (Invitrogen). PCR reactions were performed in a 12.5 Al volume with 50 ng of template and 50 ng of gene specific sense and antisense primer per reaction, under the following cycling conditions: 45°C for 30 min, 94°C for 2 min; 30 cycles: 94°C for 15 s, 55°C for 30 s, 68°C for 40 s; 72°C for 7min. For semi-quantitative RT-PCR analysis, the levels of expression of the target genes were normalized to the levels of the ubiquitously expressed ribosomal subunit *RPL-19*. Gene specific primers used were: for mouse *RPL-19* yielding a 556 bp product and *Alk6* yielding a 292 bp product (Lamm et al., 2001); for *mAlk2*, sense, 5′-GGAAAGTTGTCTGTGTGGAT-3′, antisense, 5′-TCTGTTCTGACAACCAGTCA-3′ yielding a 283 bp product; for *mAlk3*, sense, 5′-ATTGAAAATCAGAGCCTTCA-3′, antisense, 5′-CAGACTTGGACCAGAAGAAG-3′ yielding a 219 bp product; for *mNotch1*, sense, 5′-CCATCCTTACAGGAACCATA-3′, antisense, 5′-TACTGTGAAATCAACACGGA-3′ yielding a 293 bp product; for *mDll1*, sense, 5′-GCAGGTACAGGAGAAGTCGT-3′, antisense, 5′-GCTTCTATGGCAAGGTCTGT-3′ yielding a 339 bp product; *mJag1*, sense, 5′-GCTGGCAATCAGATTCTTAC-3′, antisense, 5′-AACATCGATGACTGTTCTCC-3′ yielding a 180 bp product; and for *mJag2*, sense, 5′-CGTGAATATGACCACTTCCT-3′; antisense, 5′-GACTCTTTCTCCTGCATCTG-3′ yielding a 297 bp product.

Explant cultures

Explants of embryonic and postnatal urogenital sinus were dissected in PBS and grown on 0.4 μm filters in 12 mm Transwell Plates (Corning Incorporated) in defined DMEM/F12 (1:1) medium supplemented with 2% ITS (12.5 μg/ml insulin, 12.5 μg/ml trasferrin, 12.5 ng/ml selenious acid, 2.5 mg/ml bovine serum albumin, 0.7 μg/ml linoleic acid, Collaborative Biomedical Products); non-essential amino acids (Gibco); 1% antibiotic-antimycotic (100 units/ml penicillin, 100 μg/ml streptomycin, 0.25 μg/ml amphoteracin (Gibco)) and with 10^{-8} M R1881 androgen analog (Sigma). Recombinant human BMP7 and FGF10 were obtained from R&D Systems Inc. (Minneapolis, MN). Medium was replaced every 36 h.

To separate the epithelium and mesenchyme, the urogenital sinus tissue was treated with 2.5% trypsin, 0.5% pancreatin in Tyrode solution (Weaver et al., 2000) for 30 min at room temperature, then neutralized with 10% FBS in DMEM/F12 for 30 min on ice. Distal and proximal mesenchyme, and the epithelium of the urogenital sinus were teased away with tungsten needles.

Results

BMP7 is expressed dynamically during prostate development

BMP7^{lacZ} reporter strain has been made and used previously for analysis of *BMP7* expression and function in the ureteric bud and nephrogenic mesenchyme during development of the kidney (Godin et al., 1998; Dudley et al., 1999). Our analysis of the lower urogenital system in *BMP7*$^{lacZ/+}$ mice uncovered that *BMP7* is expressed in all lobes of the mouse prostate gland: the anterior (AP), dorso-lateral (DLP) and ventral (VP) prostates (Figs. 1E-G). We confirmed, using *BMP7* probe by whole mount in situ hybridization of wild type urogenital sinus, that *BMP7*^{lacZ} expression reflects that of the endogenous gene (not shown). *BMP7*$^{lacZ/+}$ mice develop normally (Godin et al., 1998 and our data) and *BMP7*$^{lacZ/+}$ heterozygous prostates are

morphologically and histologically indistinguishable from wild type. Thus, further analysis of *BMP7* expression during development of the mouse prostate gland was carried out in the $BMP7^{lacZ}$ reporter strain by staining for β-galactosidase activity (Godin et al., 1998). To better understand morphogenesis of the prostate, we defined the following stages in prostate development, similar to those described for the submandibular gland (Jaskoll et al., 2002): E16-E17, formation of the prebud placodes of the prostate as thickened domains of the urogenital epithelium (Fig. 2A); E17, formation of the initial buds as invaginations of the prebud placodes into mesenchyme (Figs. 2A, B); E17-E19, extension of the initial buds through the mesenchyme (Fig. 1C); E19-P1, pseudoglandular stage—formation of stratified epithelium; P1, formation of the ductal canal (canalization) and initiation of postnatal branching (Fig. 1D). We found that low levels of $BMP7^{lacZ}$ are first detectable in the urogenital sinus mesenchyme at E15 (Fig. 1A), i.e. about 48 h prior to the appearance of the first initial buds at E17 (Figs. 2A, B). At E17, $BMP7^{lacZ}$ is upregulated in the urogenital mesenchyme, in particular in the dorsal area (Fig. 1B). Analysis of transverse sections shows that at E17 thickening of the urogenital epithelium is seen along the mesenchymal-epithelial boundary (Fig. 2A, arrowhead), suggesting formation of the prebud placodes. At E17, $BMP7^{lacZ}$ expression is concentrated to a narrow layer of mesenchyme immediately adjacent to the multilayered pseudostratified urogenital sinus epithelium (Figs. 2A-D). At E17, the initial buds invaginate into mesenchyme (Fig. 2A, arrows). Interestingly, during formation of the initial buds, $BMP7^{lacZ}$ expression is significantly reduced in the mesenchyme immediately adjacent to the bud tips (Fig. 2A, arrows). Notably, $BMP7^{lacZ}$ is not expressed in the urothelium at any stages in embryogenesis (Figs. 2A-C and data not shown) or postnatally (Fig. 2E and data not shown). $BMP7^{lacZ}$ is not detectable in the prostate epithelium at the initial stages of morphogenesis, i.e. at the prebud (Fig. 2A, arrowhead) and the initial bud stages (Fig. 2A, arrows). Weak $BMP7^{lacZ}$ expression first appears in the prostate epithelium as the initial buds begin to extend (Fig. 2B, arrows) followed by upregulation at the prostate tips (Fig. 2B, arrowheads). Whole mount analysis of E18 urogenital sinus (Fig. 1C) shows high $BMP7^{lacZ}$ expression at the tips of the extending initial buds of the anterior, ventral and dorso-lateral prostates (Fig. 1C, arrows). $BMP7^{lacZ}$ expression is initially low at the bud stalks (Fig. 1C, arrowhead). Following upregulation at the epithelial tips, $BMP7^{lacZ}$ expression spreads proximally to the stalks within 24 h (compare Figs. 1C, D). In the postnatal prostate, $BMP7^{lacZ}$ is expressed in the epithelium in all prostate lobes (Figs. 1E-G). As during prostate formation in embryogenesis, during postnatal branching, $BMP7^{lacZ}$ levels are highest at the distal tips (Figs. 1I, 2E).

BMP7 expression in the mouse prostate differs from that of the seminal vesicles, also exosecretory gland in mouse, which develops adjacent to the anterior prostate (Figs. 1E, F). In the seminal vesicles, $BMP7^{lacZ}$ expression appears in the epithelium at E17 (Fig. 1B), is present transiently at the epithelial tips during postnatal branching (Figs. 1E, F) and is absent by 3 weeks of age (data not shown). In contrast, in the prostate, $BMP7^{lacZ}$ expression in the epithelium persists into adulthood (assayed up to 18 months of age, data not shown). In addition, *BMP7* is not expressed in the mesenchyme of the seminal vesicles (Fig. 1B). Those differences in *BMP7* expression may potentially reflect the different origin of the prostate and seminal vesicles: prostate epithelium and mesenchyme are derived from the urogenital sinus, whereas seminal vesicles originate from the Wolfian ducts.

During development of the lungs, part of *BMP4*-expressing mesenchyme undergoes differentiation into smooth muscle (Weaver et al., 2003). In contrast, we found that *BMP7* is excluded from differentiating myoblasts during prostate formation in embryogenesis (Fig. 2D) and during postnatal development (Fig. 2F). Analysis of $BMP7^{lacZ}$ and α-smooth muscle actin (sma) expression in E17 male urogenital sinus (Figs. 2C, D) showed that $BMP7^{lacZ}$-positive periurethral mesenchyme is continuous antero-posteriorly along the urethra and is separated by *LacZ*-negative mesenchyme from the sma-positive myoblasts in the distal mesenchyme.

Thus, only a subpopulation of sma-negative fibroblasts closest to the epithelium expresses *BMP7*^{lacZ} (Figs. 2C, D). In the postnatal prostate, *BMP7*^{lacZ} expression is maintained in the mesenchyme proximally to the urethra (Figs. 2E, F, arrows) and absent near the distal prostate tips (Figs. 2E, F, arrowheads). Notably, at the distal tips, smooth muscle differentiates immediately adjacent to the ductal epithelium (Fig. 2F, arrowheads).

BMP7 null anterior prostates show excessive branching

To address the function of BMP7 during prostate development, we analyzed branching morphogenesis in *BMP7*$^{lacZ/lacZ}$ null (Figs. 1J, 4F-H) and normal *BMP7*$^{lacZ/+}$ heterozygous prostates (Figs. 1I, 4D, E). Most *BMP7*$^{lacZ/lacZ}$ homozygous mice die soon after birth due to severe defects in nephrogenesis leading to kidney failure. Yet, 7-10% of *BMP7*$^{lacZ/lacZ}$ newborns survive up to 10 days (Godin et al., 1998 and our data). We compared branching of P3 *BMP7*$^{lacZ/+}$ heterozygous (Fig. 1I) and *BMP7*$^{lacZ/lacZ}$ homozygous prostate lobes (Fig. 1J) stained in whole mount with X-Gal to visualize prostate epithelium. We found that lack of functional *BMP7* allele resulted in significant increase in the number of distal tips and branching points in the anterior prostate of *BMP7*$^{lacZ/lacZ}$ null mice (compare Figs. 1I and J). The mean number of distal tips increased from 12 ± 2 (mean ± SEM, $n = 8$) in P3 *BMP7*$^{lacZ/+}$ heterozygous prostate lobes to 25 ± 3 (mean ± SEM, $n = 8$) in P3 *BMP7*$^{lacZ/lacZ}$ homozygous prostate lobes. In addition, *BMP7*$^{lacZ/lacZ}$ homozygous anterior prostates showed distinct changes in the branching pattern. At P3, wild type and *BMP7*$^{lacZ/+}$ heterozygous anterior prostates are composed of a single main trunk with non-branched secondary buds (Fig. 1I). In contrast, *BMP7*$^{lacZ/lacZ}$ null prostates undergo extensive secondary and tertiary branching at early postnatal stages acquiring a more bulky and branched ductal structure (Fig. 1J). Thus, we conclude that BMP7 signaling functions to inhibit prostate branching during normal development.

BMP7 inhibits branching morphogenesis in prostate explants

To complement *BMP7* loss-of-function studies, we investigated the effect of gain of BMP7 function in prostate in explant cultures. *BMP7*$^{lacZ/+}$ urogenital explants were isolated at P1 and cultured for 4 days in the absence or presence of recombinant BMP7 at 50, 100 and 300 ng/ml (Figs. 3A-D). We found that BMP7 inhibited formation of prostate buds in a dose-dependent manner (Figs. 3A-D, E). Growth of explants in defined medium without BMP7 treatment resulted in formation of six buds of each dorso-lateral (Fig. 3A) and ventral (not shown) prostate lobes, and a pair of anterior prostate tips (not shown). Treatment with BMP7 at 50 ng/ml resulted in 50% decrease in the number of total prostate buds (Fig. 3E, $n = 6$). Among those, we observed three to four dorso-lateral prostate tips (Fig. 3B), two to three ventral prostate tips and one or none anterior prostate lobes (not shown). Growth of seminal vesicles was not affected (Figs. 3B-D). At 100 ng/ml of BMP7 in the medium, only a single tip or a left-right pair of dorso-lateral (Fig. 3C), ventral (not shown) and anterior (Fig. 3C) prostate tips formed. At 300 ng/ml of BMP7 in the medium, dorso-lateral prostate failed to form (Fig. 3D), although a single ventral and anterior prostate bud was observed (in four of six experiments). We conclude, that increased BMP7 signaling inhibited branching morphogenesis in urogenital sinus explants.

BMP7 inhibits Hes1 expression in urogenital sinus explants

Recent studies have suggested that Notch activity during epithelial morphogenesis can be modulated by FGF and BMP signaling (Mustonen et al., 2002; Hart et al., 2003). To assay whether inhibition of branching morphogenesis in the prostate by BMP7 may be mediated by the Notch1 pathway, we first investigated the effect of recombinant BMP7 on the level of *Hes1* transcription in cultured embryonic urogenital sinus (Fig. 3F). Explants of E17 urogenital sinus were cultured in the defined medium alone for control, in the presence of recombinant

BMP7 (300 ng/ml), or the combination of BMP7 (300 ng/ml) and FGF10 (100 ng/ml), and the levels of *Hes1* mRNA were compared by semi-quantitative RT-PCR analysis (Fig. 3F). Interestingly, treatment with BMP7 decreased *Hes1* expression in the explants to trace levels (Fig. 3F, compare lanes 2 and 4), indicating that BMP7 signaling inhibited Notch1 activity in the cultured explants. FGF10 has been shown to support Notch1 activity and *Hes1* expression during morphogenesis of the pancreas, as well as in the tooth bud (Hart et al., 2003; Norgaard et al., 2003; Mustonen et al., 2002). We found that, in the urogenital explants, the combination of BMP7 and FGF10 counteracted the inhibitory effect of BMP7 and restored *Hes1* expression close to control levels (Fig. 3F, compare lanes 2 and 6). Treatment of explants with FGF10 alone had no detectable effect on the levels of *Hes1* expression (not shown). *FGF10* expression has been previously reported in the distal mesenchyme of the urogenital sinus and prostate, and is required for prostate growth (Donjacour et al., 2003). Thus, we suggest that the combination of BMP7 and FGF10 may contribute to regulation of the Notch pathway during prostate development.

Expression of Notch pathway genes during prostate development

To define the function of Notch pathway during prostate development, we analyzed nuclear localization of the cytoplasmic domain of the Notch1 receptor (cNotch1) (Figs. 4A and 5), and expression of the Notch pathway genes in the embryonic urogenital sinus by section in situ hybridization (Figs. 4B-H) and semi-quantitative RT-PCR (Fig. 4I). Examination of sections of E18 urogenital sinus showed that cNotch1 localizes to the nucleus in the urogenital epithelium adjacent to the mesenchyme (Fig. 4A). Consistently, expression of the *Notch1* receptor was detected only in the urogenital epithelium (Figs. 4B, I). Expression of *Hes1*, the downstream target of Notch1 was also restricted to the urogenital epithelium (Figs. 4C, D). In contrast, Notch1 ligands, *Dll1* (Figs. 4E, I) and *Jag1* (Fig. 4I) were found differentially expressed in the urogenital epithelium and mesenchyme. In situ hybridization revealed that *Dll1* expression is high in selected cell clusters in the urogenital epithelium (Fig. 4E). Interestingly, clusters of cells with high *Dll1* expression (Fig. 4E) coincide with areas of low cNotch1 (Fig. 4A) activity on the adjacent section, and vise versa. *Jag1* expression was also found in the urogenital mesenchyme and epithelium with highest levels in the proximal mesenchyme (Fig. 4I). RT-PCR analysis showed that *Jag2* is expressed at trace levels uniformly in the epithelium and mesenchyme (not shown). Glycosylation of the Notch1 receptor by Fringe glycosyltransferases is known to potentiate Notch1 interaction with Dll1 and can inhibit Notch1 interaction with Jag1,2 (Lei et al., 2003;Moloney et al., 2000;Panin et al., 2002). Our analysis indicates that *Lunatic* (Fig. 4F), *Maniac* (Fig. 4G) and *Radical Fringe* (Fig. 4H) are all expressed in the urogenital epithelium with higher levels at the distal epithelium, and are upregulated at the sites of forming prostate buds. Notably, the areas of highest *Fringe* expression, in particular that of *Maniac Fringe* (Fig. 4G), coincide with domains of high Notch1 activity (Figs. 4A, F-G). Thus, our analysis indicates that at the time of prostate formation Notch1 activity is localized to the discrete epithelial domains adjacent to the mesenchyme, which are potentially the sites of perspective bud formation (Fig. 4A). In addition, domains of high Notch1 activity coincide with expression of *Fringes* (Figs. 4A, F-H), and are complementary to the domains of high *Dll1* expression (Figs. 4A, E), suggesting the possibility that Notch-Delta selection mechanism may be involved in defining the positions of the prostate buds.

Relationship between cNotch1 and pSmad1 activity during prostate development

BMP7 signaling is mediated by binding to a heteromeric receptor complex, composed of type II receptors: ActRII or BmpRII, and type I receptors: Alk2 or Alk6 (Yamashita et al., 1996). Alk3 has also been shown to bind BMP7, although no downstream signaling has been recorded (Dewulf et al., 1995). To determine whether BMP7 specific receptors may function during prostate development, we assayed the expression of *Alk2*, *Alk3* and *Alk6* by semi-quantitative

RT-PCR in E17 urogenital epithelium, proximal and distal mesenchyme (Fig. 4I). We found that all three BMP7 binding receptors are expressed in embryonic urogenital epithelium. In contrast, only the *Alk6* receptor was detected in the proximal urogenital mesenchyme, whereas *Alk2* and *Alk3* are expressed in the distal mesenchyme.

Upon binding to BMP7, activation of the type I receptors results in phosphorylation and nuclear translocation of the transcription factor Smad1 (Macacias-Silva et al., 1998). To define the areas of phospho-Smad1 (pSmad1) signaling during embryonic and postnatal development of the prostate, we analyzed nuclear localization of pSmad1 on sections of E18 male urogenital sinus (Fig. 5A), and in P1 and P3 prostate (Figs. 5D, I). We found that at the time of prostate formation at E18 pSmad1 is present and localized to the nucleus in the medial layer of the embryonic urogenital epithelium (Fig. 5A). Examination of sections of $BMP7^{lacZ/+}$ E18 urogenital sinus showed that cNotch1 localizes to the nucleus at the forming prostate buds (Fig. 5B). Interestingly, overlay of the adjacent sections showed that both pSmad1 and cNotch1 signaling is present in the developing prostate buds, however, within essentially non-overlapping adjacent domains (Fig. 5C, arrows). Nuclear cNotch1 and pSmad1 localization was mutually exclusive in 95% of nuclei scored for pSmad1 signaling and 85% of nuclei scored for cNotch1 signaling, which is consistent with our RT-PCR data showing that BMP7 inhibits Notch1/Hes1 pathway in urogenital explants (Fig. 3F).

To determine the distribution of pSmad1 and cNotch1 signaling during postnatal prostate branching, we examined the sections of $BMP7^{lacZ/+}$ heterozygous prostates at P1 (Figs. 5D, E) and P3 (Figs. 5I-K). At P1, we detected high levels of nuclear pSmad1 in selected areas of the urogenital epithelium (Fig. 5D, ur), proximal mesenchyme (Fig. 5D, pm), as well as in the distal mesenchyme (Fig. 5D, dm), which differentiates into smooth muscle. In contrast, cNotch1 was localized to the nuclei only in the distal prostate tips (Fig. 5E). At P3, pSmad1 signaling is high in the proximal urogenital epithelium (Fig. 5I, ur), in selected cell clusters in prostate epithelium (Fig. 5I, arrows) and in the urogenital mesenchyme (Fig. 5I, m). At P3, cNotch1 signaling was detected in the urogenital epithelium (Fig. 5J, ur), and in selected clusters in the prostate buds (Fig. 5J, pr, arrows). Notably, as at earlier stages, domains of pSmad1 and cNotch1 signaling have little or no overlap in P3 prostate (Fig. 5K). Thus, during postnatal prostate branching as in embryogenesis, cNotch1 activity is localized to the proximal urothelium and selected clusters within forming prostate buds and distal tips, and is excluded from the domains of pSmad1 signaling.

We reported that lack of BMP7 signaling in $BMP7^{lacZ/lacZ}$ null prostates resulted in significant increase in secondary and tertiary branching in the anterior prostate lobes (Figs. 1I, J). We further compared the distribution of pSmad1 and cNotch1 signaling on the sections of P1 $BMP7^{lacZ/lacZ}$ null (Figs. 5F-H) and $BMP7^{lacZ/+}$ heterozygous prostates (Figs. 5D, E). Analysis of $BMP7^{lacZ/lacZ}$ null prostates at P1 uncovered significant changes both in pSmad1 (Fig. 5F) and cNotch1 signaling (Fig. 5G). As expected, pSmad1 signaling was significantly decreased in $BMP7^{lacZ/lacZ}$ null urogenital epithelium (Figs. 5F, H), reflecting lack of BMP7 signaling from the periurethral mesenchyme. Interestingly, pSmad1 signaling persisted in few cell clusters at the distal tips (Figs. 5F, H), likely reflecting BMP4 signaling in the distal mesenchyme (Lamm et al., 2001). Interestingly, in $BMP7^{lacZ/lacZ}$ null prostates, cNotch1 signaling was widely spread in the urogenital epithelium as well as in multiple prostate buds (Figs. 5G, H). These results indicate that loss of functional BMP7 in $BMP7^{lacZ/lacZ}$ null prostates results in derepression of cNotch1 signaling in urogenital and prostate epithelium (compare Figs. 5E and G). Thus, we suggest that cNotch1 signaling is associated with the domains of urogenital epithelium that are competent to form new prostate branches, and that BMP7 functions to restrict prostate branching by limiting the number of domains with high Notch1 activity.

Discussion

Branching morphogenesis is an ancient repetitive algorithm of induction and repression of epithelial bud formation which is used in the development of lungs and all exosecretory glands in mammals. Development of epithelial-mesenchymal organs by branching morphogenesis allows to increase luminal surface, while retaining compact volume and modular functional structure. Signaling factors, BMP, FGF and SHH have been implicated in branching morphogenesis in various organs. However, how the signaling is interpreted in the epithelium to define the bud regions is still unclear. We investigated the function of BMP7 signaling in branching morphogenesis of the mouse prostate gland, and the interaction between the BMP7 and Notch1 pathways during prostate development. We combined gain and loss of function approaches to show that BMP7 inhibits branching morphogenesis in the mouse prostate, and also interferes with Notch1 pathway in the urogenital and prostate epithelium. We further show that high Notch1 activity is associated with forming prostate buds. Based on our data, we propose a model thereby during prostate development, BMP7 signaling inhibits prostate branching, and limits the number of domains with high Notch1 activity. We discuss the possibility of involvement of the Notch selection system in defining morphogenetic domains and/or cell fate choice during branching morphogenesis.

BMP7 is regulated dynamically during prostate development

Previous studies have shown that BMP7 is expressed in the ureteric bud and is important for development of the kidney (Dudley et al., 1995, 1999; Godin et al., 1998). Here, we show that *BMP7* is expressed during development of the male urogenital sinus, and present evidence that BMP7 contributes to branching morphogenesis in the prostate gland. The dynamics of *BMP7* expression in the embryonic urogenital sinus provides the first indication of the importance of BMP7 function in the prostate development: first, *BMP7* is expressed early in development in the urogenital mesenchyme, at E15, i.e. at least 48 h prior to the initiation of prostate morphogenesis; second, the initial *BMP7* expression is concentrated to a narrow layer of the urogenital mesenchyme adjacent to the epithelium which subsequently undergoes branching morphogenesis; and third, during branching morphogenesis in the prostate, *BMP7* expression dynamically shifts between the adjacent compartments of the epithelium and mesenchyme, and from the tips to the stalks of the epithelial ducts. At the beginning of prostate development at E17, at the prebud stage, *BMP7* is not expressed in the urogenital epithelium, but expression is high in the periurethral mesenchyme. At the initial bud stage, *BMP7* expression is decreased in the mesenchyme adjacent to the bud tips. At the late initial bud stage, *BMP7* expression appears in the prostate epithelium. During the bud extension stage, *BMP7* is upregulated at the bud tips, and is extended towards the stalks during the pseudoglandular stage. This dynamic changes in *BMP7* expression may be regulated by short-range ligands signaling between the epithelium and the mesenchyme, and within the epithelial sheet. Although the identity of those ligands is currently unknown, potential candidates include SHH (Podlasek et al., 1999), the Wnt molecules (Soshnikova et al., 2003; Kuschel et al., 2003) and androgens (Berman et al., 2004; Thomas et al., 1998). Upregulation of SHH and its putative downstream effector, the NKX3.1 homeobox protein, has been reported in the urogenital and prostate epithelium (Kim et al., 2002; Podlasek et al., 1999). Yet, in our experiments, recombinant SHH failed to affect *BMP7* expression in cultured urogenital sinus (our unpublished data). We have also detected nuclear localized β-catenin in the epithelium of the prostate tips and in the interbud mesenchyme (our unpublished data), indicating that Wnt/h-catenin pathway may be important in prostate development. We think that androgens are unlikely to regulate *BMP7* expression during prostate development, as *BMP7* is also expressed during branching morphogenesis in the female clitorial gland (our unpublished data). However, it is possible that androgens may contribute to the maintenance of *BMP7* expression in the

androgen-dependent prostate epithelium in the adult, as we have observed continued *BMP7* expression in the prostate at least up to 18 months of age.

BMP7 inhibits branching morphogenesis in the prostate

We have found that loss of functional BMP7 in *BMP7*$^{lacZ/lacZ}$ null anterior prostates significantly increases branching. Concurrently, treatment of explanted urogenital tissue with recombinant BMP7 inhibited formation of prostate buds in a dose-dependent manner. Together, these findings strongly suggest that BMP7 inhibits formation of the new branching sites in the urogenital and prostate epithelium. How is BMP7 signaling translated in the prostate epithelium to limit the number of the prebud sites? One possibility is that during prostate development BMP7 signaling is spatially modulated by the BMP extracellular antagonists, such as follistatin and noggin (Weaver et al., 2003; Morgan et al., 2003). Expression of follistatin, the major BMP7 antagonist has been detected in the prostate epithelium in newborn rats (Cancilla et al., 2001), and expression of noggin has been reported in the penile mesenchyme in mouse (Morgan et al., 2003). Another possibility is that BMP may function in branching morphogenesis by affecting cell survival in a context-dependent manner. For instance, BMP7 signaling is necessary for survival of the pronephrogeneic mesenchyme during development of the kidney (Dudley et al., 1999), while BMP7 is required for programmed cell death during development of the limbs and external genitalia (Katagiri et al., 1998; Morgan et al., 2003). Indeed, the increased number of prostate buds in *BMP7* null mice suggests that lack of BMP7 signaling may favor selective survival of the epithelial progenitors with particular morphogenetic fates.

BMP7 inhibits Notch1 pathway in the prostate epithelium

In this study, we explored the relationship between BMP7 signaling and the Notch1 pathway during branching morphogenesis in the prostate. We show that high Notch1 activity is specifically associated with formation of the initial buds in the prostate in embryogenesis and postnatally. We further show that recombinant BMP7 inhibits expression of *Hes1*, the reporter of Notch1 activity, in prostate organ cultures. On the other hand, in *BMP7* null mice, increased prostate branching coincided with significant decrease of pSmad1 signaling and wide spread of Notch1 signaling in the urogenital epithelium. Together, our data indicate that BMP7 inhibits Notch1 pathway in the prostate epithelium and limits the number and size of cell clusters with high Notch1 activity. It is important to point that our data does not test directly the involvement of Notch1 in prostate morphogenesis. Although our data shows that Notch1 activity is always associated with forming prostate buds, we cannot ascertain whether Notch1 pathway may be involved in prostate morphogenesis directly, for instance in defining the bud versus interbud regions; or that Notch1 activity might contribute towards cell fate determination after the bud domain is defined by a Notch-independent mechanism. Future studies in our laboratory on Notch1 gain of function during prostate development using retroviral infections to express activated form of Notch1; and analysis of the effect of loss of Notch function in *Hes1* mice mutants will provide further evidence on Notch1 function in cell fate choice and/or branching morphogenesis in the prostate gland.

We have found that during postnatal branching, as in embryogenesis, high Notch1 activity is concentrated to the prebud epithelium, and the tips of the initial and extending prostate buds. This suggests that Notch1 pathway functions similarly during formation of the primary prostate buds, which originate at defined positions around the urethra; and during postnatal prostate branching, which occurs semi-randomly. Since appearance of secondary and tertiary prostate tips is significantly increased in *BMP7* null prostates, it is reasonable to assume that lack of BMP7 signaling during postnatal branching results in an environment permissive for formation of the additional prostate buds. However, we cannot completely exclude the possibility that it is the lack of BMP7 signaling earlier, at E14-E17 in embryogenesis, that allows specification

of a larger number of hypothetical bud progenitor cells that give rise to additional branches postnatally.

Since BMP7 is expressed throughout the periurethral mesenchyme in the urogenital sinus, our model suggests that the inhibitory effect of BMP7 is locally downregulated and/or compensated by another factor for bud outgrowth to begin. The factors promoting bud extension during branching morphogenesis in the prostate may be, for instance, FGF10 or SHH. In the lungs, FGF10 has been shown to promote budding and proliferation of the epithelium, and was suggested to compensate for the inhibitory effect of BMP4 in the buds at short-range; whereas in the interbud regions, the restrictive effect of BMP4 is thought to predominate at long distance (Hogan, 1999). In the prostate, *FGF10* is expressed similarly as in lungs, and is localized to the mesenchyme adjacent to prostate tips during postnatal branching (Bellusci et al., 1997; Donjacour et al., 2003). We have shown that BMP7 alone inhibited Notch1/Hes1 activity in cultured urogenital sinus, while explants grown in the presence of FGF10 maintained *Hes1* expression in culture even when treated with BMP7. Thus, our data indicate that FGF10 can maintain activity of the Notch1 pathway downstream or independent of BMP7 signaling.

A model for relationship between branching morphogenesis and proximal-distal cell fate choice

Since cell autonomous Notch1 activity is high in the initial buds and at the distal prostate tips, we hypothesize that during branching morphogenesis in the prostate Notch1/Hes1 activity may define the epithelium of the prebud placode and the distal epithelial fates. This hypothesis is in support of the studies of Notch1 function in morphogenesis and cell fate specification in the lungs, gut and pancreas. Constitutive Notch1 activity in the pancreas has been shown to oppose proximal endocrine differentiation while favoring maintenance of the progenitor population and branching morphogenesis (Hald et al., 2003). Deficiencies in the Notch pathway in *Hes1*$^{-/-}$ lungs result in broader domains of proximal epithelium with *Dll1*+ and *Mash1*+ neuroendocrine fates (Ito et al., 2000). Similarly, *Hes1*$^{-/-}$ embryos show premature and excessive differentiation of the proximal endocrine epithelium in the pancreas, stomach and intestine (Jensen et al., 2000). Loss of *Hes1* results in loss of enterocytes in the intestine, that compose the distal epithelium of the villi, and causes hypoplasia in the pancreas (de Santa Barbara et al., 2003; Jensen et al., 2000). Thus, we suggest that in the urogenital and prostate epithelium, as in other primitive gut derivatives, *Notch1* activity suppresses the proximal epithelial fates and favors distal outgrowth of the epithelial ducts and distal fate specification.

During branching morphogenesis in the lung, the properties of the distal epithelium include the ability to respond to FGF10 with increased cell proliferation and extension distally towards the source of FGF10 (Weaver et al., 2000). In embryogenesis, FGF10 is expressed in the distal mesenchyme of the urogenital sinus and is required for the development of the prostate, ampulatory and bulbourethral glands, and the seminal vesicles (Donjacour et al., 2003). Our data indicate that FGF10 functions to maintain Notch1/Hes1 activity during prostate development. FGF10 counteracted the inhibitory effect of BMP7 on *Hes1* expression during prostate growth in culture, while urogenital explants treated with FGF10 alone maintained *Hes1* expression similar to that of untreated samples. Our data are in support of the studies in pancreas, where FGF10 has been suggested to promote survival and proliferation of the pancreatic progenitor cells, which co-express *Notch1,2* receptors, the Notch ligands *Jag1,2* and *Hes1* (Hart et al., 2003; Norgaard et al., 2003). We hypothesize that during branching morphogenesis in the prostate FGF10 may function to maintain the domains of high Notch1/Hes1 activity at the distal tip epithelium, for instance, by promoting cell division in clusters with high Notch1/Hes1 activity.

Based on our data and studies by others reviewed in this section, we propose the following model to describe branching morphogenesis in the mouse prostate gland (Fig. 6): (1) domains

of high Notch1 activity are associated with forming prostate buds and with distal tip epithelium; domains of low Notch1 activity are associated with interbud epithelium and may contribute to proximal epithelial fates; (2) BMP7 signaling inhibits formation of the new prostate buds, and limits the number of domains with high Notch1 activity; (3) FGF10 may function to promote extension of the prostate tips by favoring proliferation of the bud epithelium which exhibits high Notch1 activity.

Relationship between BMP in prostate development

Combinatorial action and partial redundancy of function for various BMPs has been suggested previously based on heterodimer formation (Suzuki et al., 1997a,b), and on the basis of early lethality of trans-heterozygous BMP4-BMP7 and BMP5-BMP7 mice (Katagiri et al., 1998; Solloway and Robertson, 1999). It has been reported that haploinsufficiency for *BMP4* increases prostate branching (Lamm et al., 2001). In addition, *BMP7* and *BMP4*, and their respective receptors, *Alk2*, *Alk4* and *Alk6*, share partially overlapping expression in the embryonic urogenital sinus and postnatal prostate (Lamm et al., 2001; and this study). Thus, BMP4 and BMP7 may have related and overlapping functions in regulation of prostate branching. Yet, our analysis of prostate morphogenesis, and pSmad1 and cNotch1 signaling in *BMP7* null prostate gland, allows to delineate the function of BMP7 in prostate development. We show that increase in prostate branching in *BMP7* null prostates is accompanied with dramatic decrease in pSmad1 signaling in the urogenital epithelium in spite of presence of BMP4 in the mesenchyme (Lamm et al., 2001). This indicates that *BMP7* expressed in the periurethral mesenchyme plays an essential role in prostate development. We present evidence that Notch1 signaling becomes derepressed in *BMP7* null urogenital and prostate epithelium, thereby showing that BMP7 signaling is essential for restricting domains of Notch1 activity. At the same time, our data shows that, in *BMP7* null prostates, pSmad1 signaling is present at the distal tip epithelium, presumably reflecting BMP4 signaling (Lamm et al., 2001). That corroborates the hypothesis that BMP4 and BMP7 function in collaboration to restrict postnatal prostate branching. Expression of *BMP2* and *BMP5* has also been reported in the urogenital sinus and postnatal prostate (King et al., 1994; Luo et al., 2002). BMP2, a close homologue of BMP4, has been reported to affect branching morphogenesis of the ureteric bud in culture (Bush et al., 2004). However, *BMP2* is expressed in the urogenital sinus at very low level (Lamm et al., 2001) and, thus, it is unlikely to significantly contribute to branching morphogenesis in the prostate. Expression of *BMP5*, a close homologue of *BMP7*, has been reported in the mesenchyme adjacent to the bladder epithelium in embryogenesis (King et al., 1994) and in the prostate postnatally (Luo et al., 2002). Thus, future studies are needed to determine the potential function of BMP5 and, possibly, BMP2 in the development of the prostate, bladder and other components of the lower urogenital system.

Acknowledgments

Probes were generously donated by Drs. Janet Rossant (*Notch1*), Achim Gossler (*Dll1*), Francois Guillemot (*Hes1*, *Lunatic*, *Maniac*, *Radical Fringes*). We are very grateful to Elizabeth Robertson for the gift of $BMP7^{lacZ}$ mouse line and *BMP7* probe. We thank Charlotte Dean and Lee Niswander for helpful discussions and critical reading of the manuscript. This work was supported by NIH NIDDDK grants DK056170 to PW, DKO7775 to the Department of Urology and DK068007 to IG.

References

Abate-Shen C, Shen MM. Molecular genetics of prostate cancer. Genes Dev 2000;14:2410–2434. [PubMed: 11018010]

Anderson DJ, Groves A, Lo L, Ma Q, Rao M, Shah NM, Sommer L. Cell lineage determination and the control of neuronal identity in the neural crest. Cold Spring Harbor Symp. Quant. Biol 1997;62:493–504. [PubMed: 9598383]

Artavanis-Tsakonas S, Rand MD, Lake RJ. Notch signaling: cell fate control and signal integration in development. Science 1999;284:770–776. [PubMed: 10221902]

Bellusci S, Grindley J, Emoto H, Itoh N, Hogan BL. Fibroblast growth factor 10 (FGF10) and branching morphogenesis in the embryonic mouse lung. Development 1997;124:4867–4878. [PubMed: 9428423]

Berman DM, Desai N, Wang X, Karhadkar SS, Reynon M, Abate-Shen C, Beachy PA, Shen MM. Roles for Hedgehog signaling in androgen production and prostate ductal morphogenesis. Dev. Biol 2004;267:387–398. [PubMed: 15013801]

Bush KT, Sakurai H, Steer DL, Leonard MO, Sampogna RV, Meyer TN, Schwesinger C, Qiao J, Nigam SK. TGF-beta superfamily members modulate growth, branching, shaping, and patterning of the ureteric bud. Dev. Biol 2004;266:285–298. [PubMed: 14738877]

Cancilla B, Jarred RA, Wang H, Mellor SL, Cunha GR, Risbridger GP. Regulation of prostate branching morphogenesis by activin A and follistatin. Dev. Biol 2001;237:145–158. [PubMed: 11518512]

Crowe R, Henrique D, Ish-Horowicz D, Niswander L. A new role for Notch and Delta in cell fate decisions: patterning the feather array. Development 1998;125:767–775. [PubMed: 9435296]

de Santa Barbara P, van den Brink GR, Roberts DJ. Development and differentiation of the intestinal epithelium. Cell. Mol. Life Sci 2003;60:1322–1332. [PubMed: 12943221]

Dewulf N, Verschueren K, Lonnoy O, Moren A, Grimsby S, Vande Spiegle K, Miyazono K, Huylebroeck D, Ten Dijke P. Distinct spatial and temporal expression patterns of two type I receptors for bone morphogenetic proteins during mouse embryogenesis. Endocrinology 1995;136:2652–2663. [PubMed: 7750489]

Donjacour AA, Thomson AA, Cunha GR. FGF-10 plays an essential role in the growth of the fetal prostate. Dev. Biol 2003;261:39–54. [PubMed: 12941620]

Dudley AT, Lyons KM, Robertson EJ. A requirement for bone morphogenetic protein-7 during development of the mammalian kidney and eye. Genes Dev 1995;22:2795–2807. [PubMed: 7590254]

Dudley AT, Godin RE, Robertson EJ. Interaction between FGF and BMP signaling pathways regulates development of metanephric mesenchyme. Genes Dev 1999;13:1601–1613. [PubMed: 10385628]

Economides KD, Capecchi MR. Hoxb13 is required for normal differentiation and secretory function of the ventral prostate. Development 2003;130:2061–2069. [PubMed: 12668621]

Freestone SH, Marker P, Grace OC, Tomlinson DC, Cunha GR, Harnden P, Thomson AA. Sonic hedgehog regulates prostatic growth and epithelial differentiation. Dev. Biol 2003;264:352–362. [PubMed: 14651923]

Foster BA, Evangelou A, Gingrich JR, Kaplan PJ, DeMayo F, Greenberg NM. Enforced expression of FGF-7 promotes epithelial hyperplasia whereas a dominant negative FGFR2iiib promotes the emergence of neuroendocrine phenotype in prostate glands of transgenic mice. Differentiation 2002;70:624–632. [PubMed: 12492503]

Godin RE, Takaesu NT, Robertson EJ, Dudley AT. Regulation of BMP7 expression during kidney development. Development 1998;125:3473–3482. [PubMed: 9693150]

Gradwohl G, Dierich A, LeMeur M, Guillemot F. Neurogenin3 is required for the development of the four endocrine cell lineages of the pancreas. Proc. Natl. Acad. Sci. U. S. A 2000;97:1607–1611. [PubMed: 10677506]

Gubbay J, Vivian N, Economou A, Jackson D, Goodfellow P, Lovell-Badge R. Inverted repeat structure of the Sry locus in mice. Proc. Natl. Acad. Sci. U. S. A 1992;89:7953–7957. [PubMed: 1518820]

Hald J, Hjorth JP, German MS, Madsen OD, Serup P, Jensen J. Activated Notch1 prevents differentiation of pancreatic acinar cells and attenuate endocrine development. Dev. Biol 2003;260:426–437. [PubMed: 12921743]

Hart A, Papadopoulou S, Edlund H. Fgf10 maintains Notch activation, stimulates proliferation, and blocks differentiation of pancreatic epithelial cells. Dev. Dyn 2003;228:185–193. [PubMed: 14517990]

Hogan BL. Morphogenesis. Cell 1999;96:225–233. [PubMed: 9988217]

Hu Y, Ippolito JE, Garabedian EM, Humphrey PA, Gordon JI. Molecular characterization of a metastatic neuroendocrine cell cancer arising in the prostates of transgenic mice. J. Biol. Chem 2002;277:44462–44474. [PubMed: 12228243]

Jaskoll T, Zhou YM, Chai Y, Makarenkova HP, Collinson JM, West JD, Hajihosseini MK, Lee J, Melnick M. Embryonic submandibular gland morphogenesis: stage-specific protein localization of FGFs, BMPs, Pax6 and Pax9 in normal mice and abnormal SMG phenotypes in FgfR2-IIIc(+/Delta), BMP7 (-/-) and Pax6(-/-) mice. Cells Tissues Organs 2002;170:83–98. [PubMed: 11731698]

Jena N, Martin-Seisdedos C, McCue P, Croce CM. BMP7 null mutation in mice: developmental defects in skeleton, kidney, and eye. Exp. Cell Res 1997;230:28–37. [PubMed: 9013703]

Jensen J, Pedersen EE, Galante P, Hald J, Heller RS, Ishibashi M, Kageyama R, Guillemot F, Serup P, Madsen OD. Control of endodermal endocrine development by Hes-1. Nat. Genet 2000;24:36–44. [PubMed: 10615124]

Ito T, Udaka N, Yazawa T, Okudela K, Hayashi H, Sudo T, Guillemot F, Kageyama R, Kitamura H. Basic helix-loop-helix transcription factors regulate the neuroendocrine differentiation of fetal mouse pulmonary epithelium. Development 2000;127:3913–3921. [PubMed: 10952889]

Katagiri T, Boorla S, Frendo JL, Hogan BL, Karsenty G. Skeletal abnormalities in doubly heterozygous Bmp4 and Bmp7 mice. Dev. Genet 1998;22:340–348. [PubMed: 9664686]

Kim MJ, Bhatia-Gaur R, Banach-Petrosky WA, Desai N, Wang Y, Hayward SW, Cunha GR, Cardiff RD, Shen MM, Abate-Shen C. Nkx3.1 mutant mice recapitulate early stages of prostate carcinogenesis. Cancer Res 2002;62:2999–3004. [PubMed: 12036903]

King JA, Marker PC, Seung KJ, Kingsley DM. BMP5 and the molecular, skeletal, and soft-tissue alterations in short ear mice. Dev. Biol 1994;166:112–122. [PubMed: 7958439]

Knecht AK, Good PJ, Dawid IB, Harland RM. Dorsal-ventral patterning and differentiation of noggin-induced neural tissue in the absence of mesoderm. Development 1995;121:1927–1935. [PubMed: 7601005]

Kuschel S, Ruther U, Theil T. A disrupted balance between Bmp/Wnt and Fgf signaling underlies the ventralization of the Gli3 mutant telencephalon. Dev. Biol 2003;260:484–495. [PubMed: 12921747]

Lamm ML, Podlasek CA, Barnett DH, Lee J, Clemens JQ, Hebner CM, Bushman W. Mesenchymal factor bone morphogenetic protein 4 restricts ductal budding and branching morphogenesis in the developing prostate. Dev. Biol 2001;232:301–314. [PubMed: 11401393]

Lei L, Xu A, Panin VM, Irvine KD. An *O*-fucose site in the ligand binding domain inhibits Notch activation. Development 2003;130:6411–6421. [PubMed: 14627724]

Luo J, Dunn T, Ewing C, Sauvageot J, Chen Y, Trent J, Isaacs W. Gene expression signature of benign prostatic hyperplasia revealed by cDNA microarray analysis. Prostate 2002;51:189–200. [PubMed: 11967953]

Macacias-Silva M, Hoodless PA, Tang SJ, Buchwald M, Wrana JL. Specific activation of Smad1 signaling pathways by the BMP7 type I receptor, ALK2. J. Biol. Chem 1998;273:628–636.

Marker PC, Donjacour AA, Dahiya R, Cunha GR. Hormonal, cellular, and molecular control of prostatic development. Dev. Biol 2003;253:165–174. [PubMed: 12645922]

Moloney DJ, Panin VM, Johnston SH, Chen J, Shao L, Wilson R, Wang Y, Stanley P, Irvine KD, Haltiwanger RS, Vogt TF. Fringe is a glycosyltransferase that modifies Notch. Nature 2000;406:369–375. [PubMed: 10935626]

Morgan EA, Nguyen SB, Scott V, Stadler HS. Loss of Bmp7 and Fgf8 signaling in Hoxa13-mutant mice causes hypospadia. Development 2003;130:3095–3109. [PubMed: 12783783]

Murtaugh LC, Stanger BZ, Kwan KM, Melton DA. Notch signaling controls multiple steps of pancreatic differentiation. Proc. Natl. Acad. Sci. U. S. A 2003;100:14920–14925. [PubMed: 14657333]

Mustonen T, Tummers M, Mikami T, Itoh N, Zhang N, Gridley T, Thesleff I. Lunatic fringe, FGF, and BMP regulate the Notch pathway during epithelial morphogenesis of teeth. Dev. Biol 2002;248:281–293. [PubMed: 12167404]

Norgaard GA, Jensen JN, Jensen J. FGF10 signaling maintains the pancreatic progenitor cell state revealing a novel role of Notch in organ development. Dev. Biol 2003;264:323–338. [PubMed: 14651921]

Ohtsuka T, Ishibashi M, Gradwohl G, Nakanishi S, Guillemot F, Kageyama R. Hes1 and Hes5 as Notch effectors in mammalian neuronal differentiation. EMBO J 1999;18:2196–2207. [PubMed: 10205173]

Panin VM, Shao L, Lei L, Moloney DJ, Irvine KD, Haltiwanger RS. Notch ligands are substrates for protein *O*-fucosyltransferase-1 and Fringe. J. Biol. Chem 2002;277:29945–29952. [PubMed: 12036964]

Parr BA, Shea MJ, Vassileva G, McMahon AP. Mouse Wnt genes exhibit discrete domains of expression in the early embryonic CNS and limb buds. Development 1993;119:247–261. [PubMed: 8275860]

Podlasek CA, Barnett DH, Clemens JQ, Bak PM, Bushman W. Prostate development requires Sonic hedgehog expressed by the urogenital sinus epithelium. Dev. Biol 1999;209:28–39. [PubMed: 10208740]

Post LC, Ternet M, Hogan BL. Notch/Delta expression in the developing mouse lung. Mech. Dev 2000;98:95–98. [PubMed: 11044610]

Robinson EJ, Neal DE, Collins AT. Basal cells are progenitors of luminal cells in primary cultures of differentiating human prostatic epithelium. Prostate 1998;37:149–160. [PubMed: 9792132]

Settle S, Marker P, Gurley K, Sinha A, Thacker A, Wang Y, Higgins K, Cunha G, Kingsley DM. The BMP family member Gdf7 is required for seminal vesicle growth, branching morphogenesis, and cytodifferentiation. Dev. Biol 2001;234:138–150. [PubMed: 11356025]

Small D, Kovalenko D, Kacer D, Liaw L, Landriscina M, Di Serio C, Prudovsky I, Maciag T. Soluble Jagged 1 represses the function of its transmembrane form to induce the formation of the Src-dependent chord-like phenotype. J. Biol. Chem 2001;276:32022–32030. [PubMed: 11427524]

Solloway MJ, Robertson EJ. Early embryonic lethality in Bmp5;Bmp7 double mutant mice suggests functional redundancy within the 60A subgroup. Development 1999;126:1753–1768. [PubMed: 10079236]

Soshnikova N, Zechner D, Huelsken J, Mishina Y, Behringer RR, Taketo MM, Crenshaw EB III, Birchmeier W. Genetic interaction between Wnt/beta-catenin and BMP receptor signaling during formation of the AER and the dorsal-ventral axis in the limb. Genes Dev 2003;17:1963–1968. [PubMed: 12923052]

Suzuki A, Kaneko E, Maeda J, Ueno N. Mesoderm induction by BMP-4 and -7 heterodimers. Biochem. Biophys. Res. Commun 1997a;232:153–156. [PubMed: 9125121]

Suzuki A, Kaneko E, Ueno N, Hemmati-Brivanlou A. Regulation of epidermal induction by BMP2 and BMP7 signaling. Dev. Biol 1997b;189:112–122. [PubMed: 9281341]

Thomas R, Anderson WA, Raman V, Reddi AH. Androgen-dependent gene expression of bone morphogenetic protein 7 in mouse prostate. Prostate 1998;37:236–245. [PubMed: 9831220]

Tomita K, Ishibashi M, Nakahara K, Ang SL, Guillemot F, Kageyama R. Mammalian hairy and enhancer of split homolog 1 regulates differentiation of retinal neurons and is essential for eye morphogenesis. Neuron 1996;16:723–734. [PubMed: 8607991]

Tsujimura A, Koikawa Y, Salm S, Takao T, Coetzee S, Moscatelli D, Shapiro E, Lepor H, Sun TT, Wilson EL. Proximal location of mouse prostate epithelial stem cells: a model of prostatic homeostasis. J. Cell Biol 2002;157:1257–1265. [PubMed: 12082083]

Wang Y, Hayward S, Cao M, Thayer K, Cunha G. Cell differentiation lineage in the prostate. Differentiation 2001;68:270–279. [PubMed: 11776479]

Weaver M, Dunn NR, Hogan BL. Bmp4 and Fgf10 play opposing roles during lung bud morphogenesis. Development 2000;127:2695–2704. [PubMed: 10821767]

Weaver M, Batts L, Hogan BL. Tissue interactions pattern the mesenchyme of the embryonic mouse lung. Dev. Biol 2003;258:169–184. [PubMed: 12781691]

Yamashita HP, Ten Dijke P, Heldin CH, Miyazono K. Bone morphogenetic protein receptors. Bone 1996;19:569–574. [PubMed: 8968021]

Yang Q, Bermingham NA, Finegold MJ, Zoghbi HY. Requirement of Math1 for secretory cell lineage commitment in the mouse intestine. Science 2001;294:2155–2158. [PubMed: 11739954]

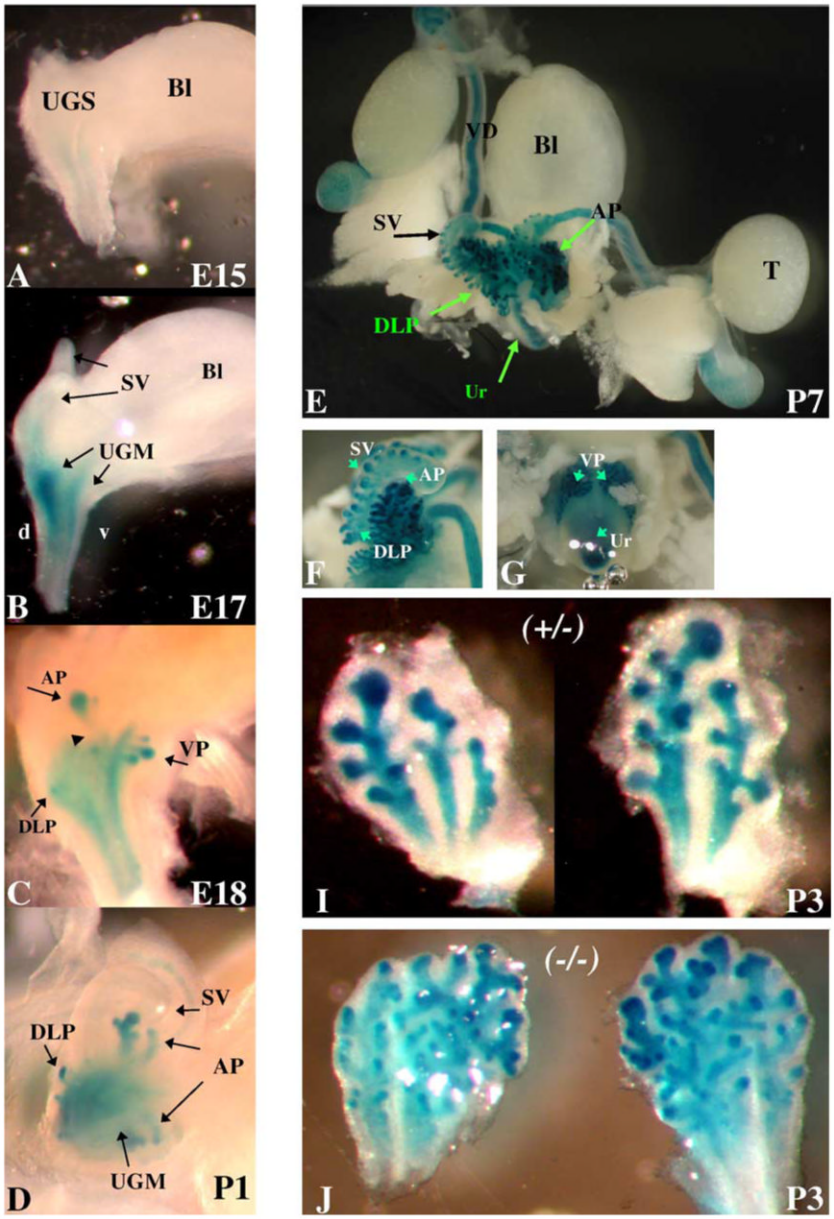

Fig. 1.

BMP7^{lacZ} expression during prostate development. (A-C) Embryonic *BMP7*$^{lacZ/+}$ male urogenital sinus stained whole mount for β-galactosidase activity (A) at E15, (B) at E17, (C) at E18. (D) *BMP7*$^{lacZ/+}$ urogenital sinus at P1 processed as in panels A-C. (A) At E15, *BMP7*^{lacZ} expression is first detectable in the periurethral mesenchyme. (B) At E17, *BMP7*^{lacZ} is strongly expressed in the urogenital mesenchyme, and appears in the epithelium of the seminal vesicles. (C) At E18, *BMP7*^{lacZ} is upregulated at the bud tips (arrowheads), and is low or absent at the bud stalks (arrows). (D) At P1, *BMP7*^{lacZ} is expressed in the prostate epithelium and in the urogenital sinus mesenchyme. (E-I) *BMP7*^{lacZ} expression in postnatal *BMP7*$^{lacZ/+}$ anterior prostate at P3 (I) and male urogenital system at P7 (E-G): (E) dorsal view, (F) lateral view, (G) ventral view. *BMP7*^{lacZ} is expressed in the epithelium and mesenchyme of the anterior (E, F, I), dorso-lateral (E, F) and ventral prostates (G); in the epithelium of the Vas Deferens, epididymus and seminal vesicles (E); and in the urethra (E, G). (I) Normal

branching pattern in P3 *BMP7*$^{lacZ/+}$ heterozygous anterior prostate. (J) Branching of P3 *BMP7*$^{lacZ/lacZ}$ null anterior prostate is increased two-fold compare to heterozygous littermate (I). Abbreviations: UGS, urogenital sinus; UGM, urogenital sinus mesenchyme; d, dorsal; v, ventral; Bl, bladder; SV, seminal vesicles; AP, anterior prostate; DLP, dorso-lateral prostate; VP, ventral prostate; VD, Vas Deferens; d, epididymus; T, testis; Ur, urethra.

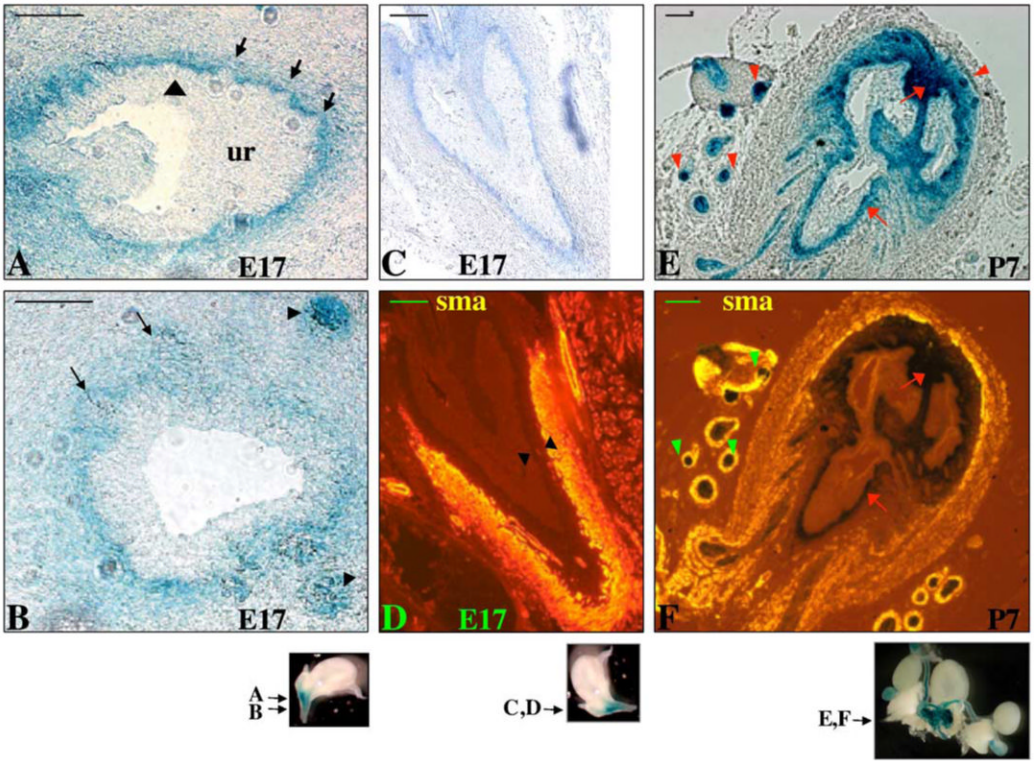

Fig. 2.

BMP7^{lacZ} expression in the prostate epithelium and mesenchyme. Paraffin sections of *BMP7*$^{lacZ/+}$ male urogenital sinus at E17 (A-D) and P5 (E, F) were stained with X-gal, and immunostained with α-smooth muscle actin (sma) (D, F). Planes of sections are indicated in the whole mount images below each panel. (A, B) Transverse section of E17 *BMP7*$^{lacZ/+}$ urogenital sinus. (A) *BMP7*^{lacZ} is expressed in the periurethral mesenchyme and absent from urothelium. Areas of thickened epithelium (prebud placodes) form along the epithelial-mesenchymal boundary (arrowhead). *BMP7*^{lacZ} is reduced in the mesenchyme adjacent to the initial buds (arrows). (B) Low levels of *BMP7*^{lacZ} appear in the prostate epithelium at the extending initial bud stage (arrows). *BMP7*^{lacZ} is upregulated at the extending prostate tips (arrowheads). (C, D) Sagittal section of *BMP7*$^{lacZ/+}$ E17 urogenital sinus. *BMP7*^{lacZ}-positive periurethral mesenchyme is separated from the myoblasts expressing smooth muscle actin (sma) by 4-6 layers of *BMP7*^{lacZ}-negative mesenchyme (arrowheads in panel D). (E, F) Transverse section of *BMP7*$^{lacZ/+}$ postnatal prostate at P5. (E) *BMP7*^{lacZ} is upregulated in the epithelium of prostate tips (arrowheads). *BMP7*^{lacZ} is maintained in the proximal mesenchyme (arrows). (F) Myoblasts expressing sma are localized adjacent to the distal prostate tips (arrowheads). In the areas proximal to the urethra, myoblasts are separated from the prostate ducts by *BMP7*^{lacZ}-positive (arrows) and *BMP7*^{lacZ}-negative mesenchyme. Scale bar, 20 μm for (A-D); 100 μm for (E, F).

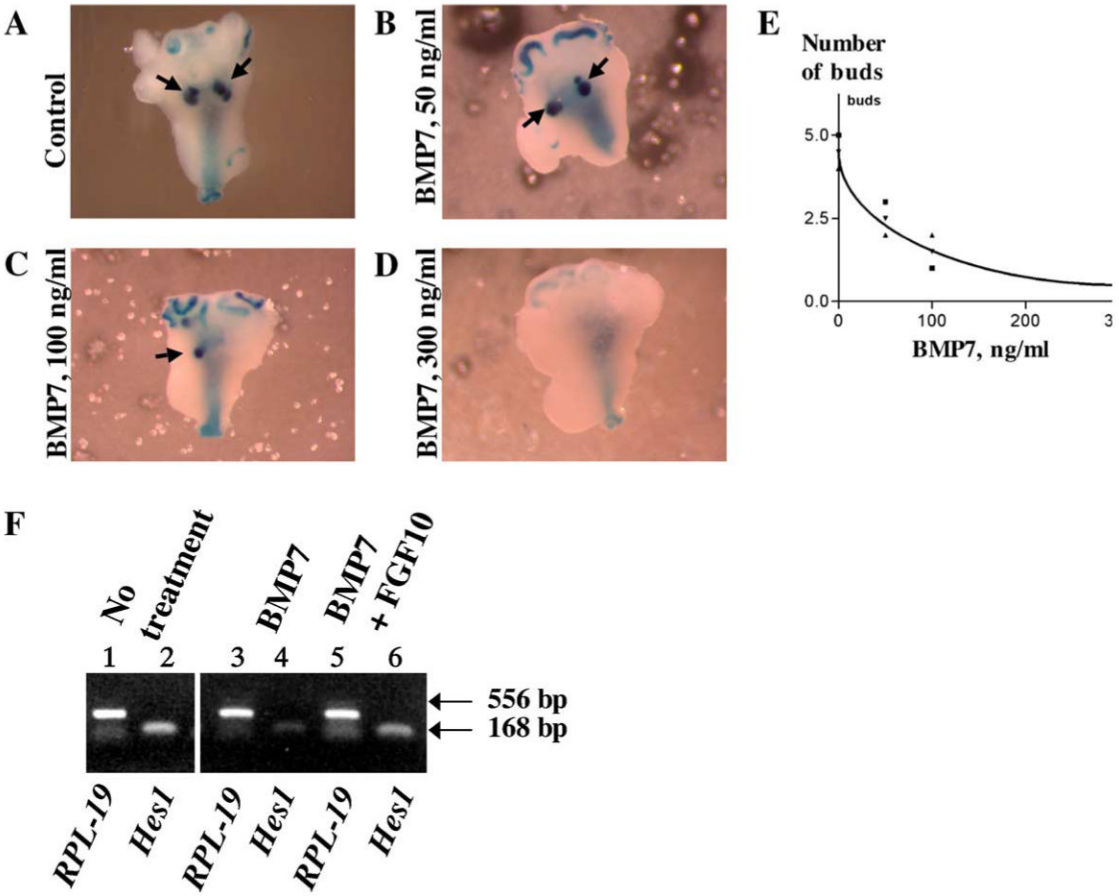

Fig. 3.

BMP7 inhibits branching morphogenesis and *Hes1* expression in prostate explants. (A-E) Recombinant human BMP7 inhibits formation of prostate buds in a dose-dependent manner. P1 *BMP7*$^{lacZ/+}$ urogenital sinus explants were cultured for 4 days in defined medium (see Materials and methods). (A) Non-treated control. (B-D) Recombinant human BMP7 (R&D Systems) was added at: (B) 50 ng/ml, (C) 100 ng/ml, (D) 300 ng/ml. Arrows are pointing to the buds of the dorso-lateral prostate. (E) Graphic representation of six experiments. The curve is drawn through the mean ± SME interval. (F) BMP7 inhibits *Hes1* expression in cultured urogenital sinus. Explants of E17 male urogenital sinus were cultured for 60 h in the absence (lanes 1, 2) and in presence of BMP7 (300 ng/ml) (lanes 3, 4); or BMP7 (300 ng/ml) combined with FGF10 (100 ng/ml) (lanes 5, 6). Levels of *Hes1* expression in the explants (lanes 2, 4 and 6) were compared by semi-quantitative RT-PCR analysis. Levels of ubiquitously expressed ribosomal subunit *RPL-19* (lanes 1, 3 and 5) are shown for semi-quantitative reference. Treatment with BMP7 inhibited *Hes1* expression in cultured prostates (compare lanes 2 and 4). Addition of FGF10 counteracted inhibitory effect of BMP7 and restored *Hes1* expression (compare lanes 2 and 6).

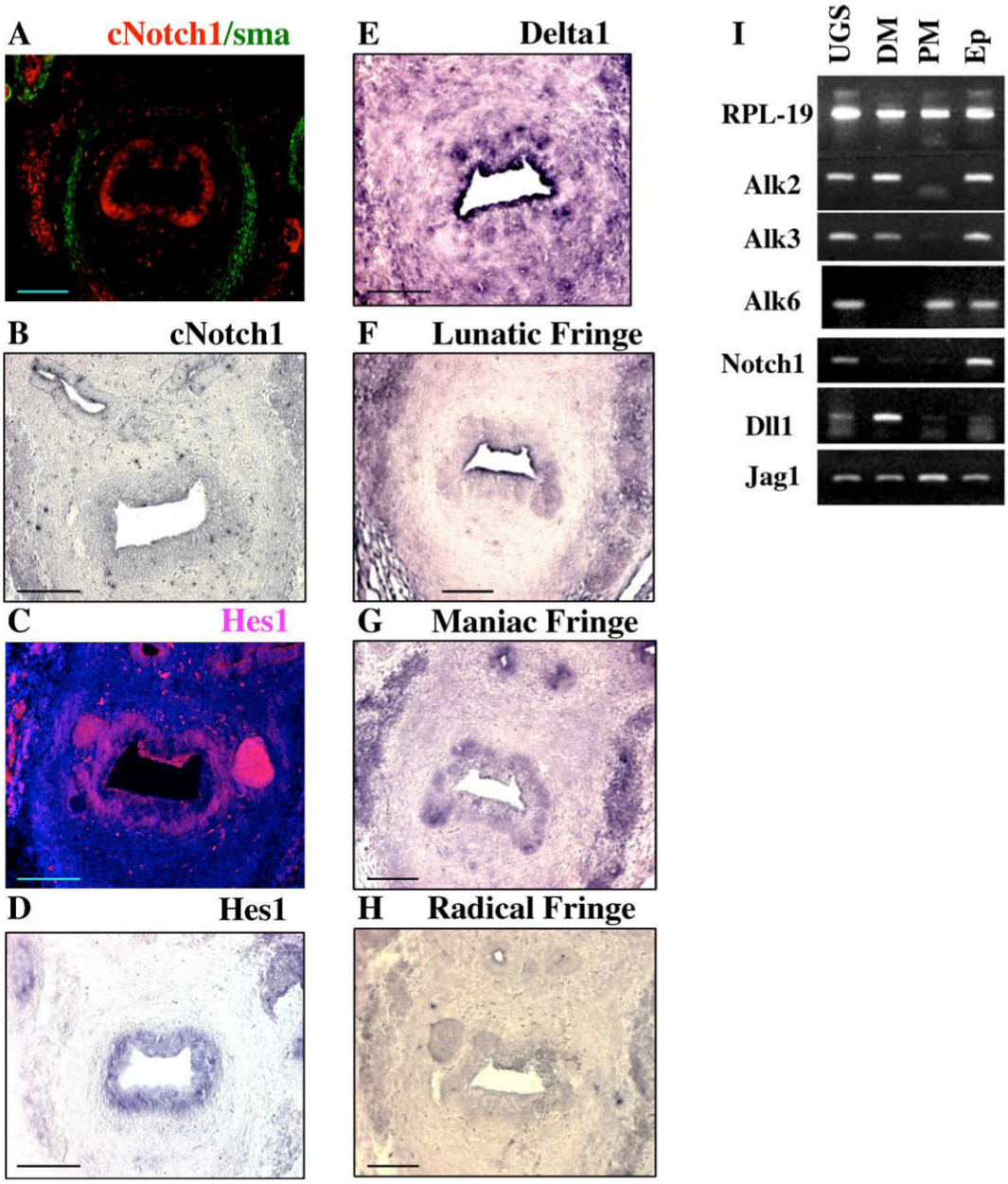

Fig. 4.

Alk and Notch pathway gene expression, and Notch1 activity in the embryonic urogenital sinus. (A) In E18 urogenital sinus, cNotch1 is localized to the nuclei in the urogenital epithelium adjacent to the mesenchyme. (B-H) In situ hybridization analysis of gene expression with digoxigenin labeled antisense RNA probes visualized with BM-purple (B, D-H) or tyramide-enhanced fluorescence (C). Expression of *Notch1* (B), *Hes1* (C, D), *Dll1* (E), *Lunatic Fringe* (F), *Maniac Fringe* (G) and *Radical Fringe* (H) is shown. Scale bar, 50 μm. (I) RT-PCR analysis of expression of *Alk* receptors, *Notch1* and Notch ligands in the whole E17 male urogenital sinus (UGS), distal mesenchyme (DM), proximal mesenchyme (PM) and urogenital epithelium (Ep). Levels of *RPL-19* are shown for semi-quantitative reference. In the urogenital epithelium, *Alk2*, *Alk3* and *Alk6* are expressed. Only *Alk6* is expressed in the proximal urogenital mesenchyme. Only *Alk2* and *Alk3* are expressed in the distal mesenchyme.

Notch1 receptor is expressed only in the urogenital epithelium. *Dll1* is expressed at low level in the epithelium and proximal mesenchyme, and at high level in the distal urogenital mesenchyme. *Jag1* is expressed in all compartments, and at highest levels in the proximal mesenchyme.

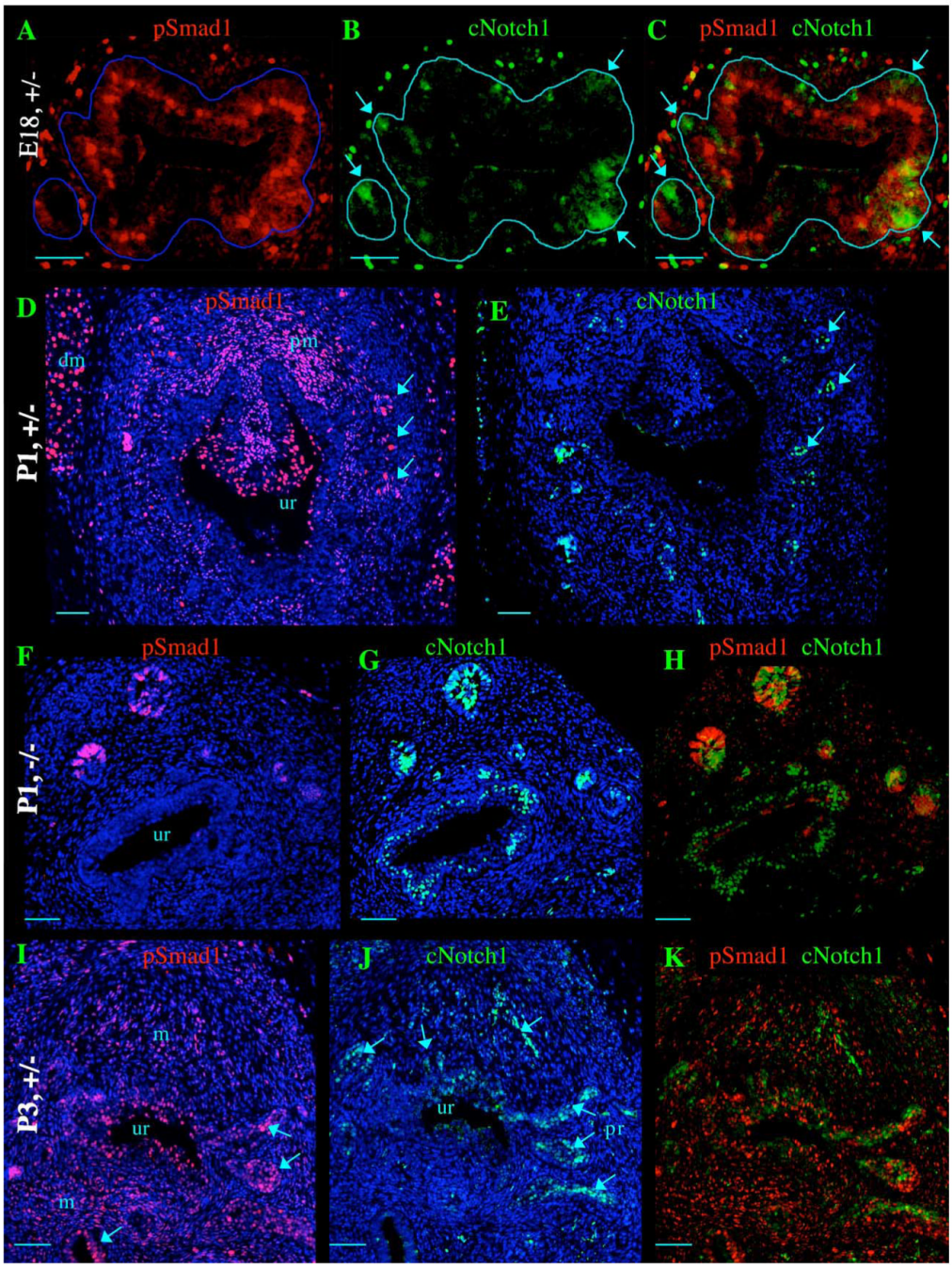

Fig. 5.

pSmad1 and cNotch1 signaling during prostate development. (A-C) Transverse sections of E18 *BMP7*$^{lacZ/+}$ heterozygous prostate. (A) pSmad1 is nuclear in the urogenital epithelium. (B) cNotch1 is localized to the nuclei of the forming prostate buds. (C) Overlay of adjacent sections A and B. Outlines of the urogenital epithelium are shown in blue. (D, E) Transverse sections of *BMP7*$^{lacZ/+}$ heterozygous prostate at P1. (D) pSmad1 is nuclear in selected areas of the urogenital epithelium (ep) and prostate buds (arrows), periurethral mesenchyme (pm) and distal mesenchyme (dm). (E) cNotch1 is localized to the nuclei at the distal tips of the prostate buds. (F-H) Transverse sections of P1 *BMP7*$^{lacZ/lacZ}$ null prostate. (F, H) pSmad1 signaling in the urogenital epithelium is significantly reduced, but is present in the distal tips.

(G, H) cNotch1 signaling is wide spread in the urogenital epithelium and prostate buds. (H) Overlay of adjacent sections F and G. (I-K) Transverse sections of *BMP7*$^{lacZ/+}$ heterozygous prostate at P3. (I) pSmad1 is nuclear in selected areas of the urogenital (ur) and prostate epithelium (arrows). pSmad1 signaling is also observed in the mesenchyme (m). (J) cNotch1 signaling in the urothelium (ur) and prostate epithelium (arrows) is localized to clusters of cells in the prostate buds and distal tips, and shows little or no overlap with pSmad1 signaling (I, K). (K) Overlay of adjacent sections I and J. DAPI staining of nuclei is shown in blue channel (D-G, I-J). Scale bar, 50 μm for sections A-H; 100 μm for sections I-K.

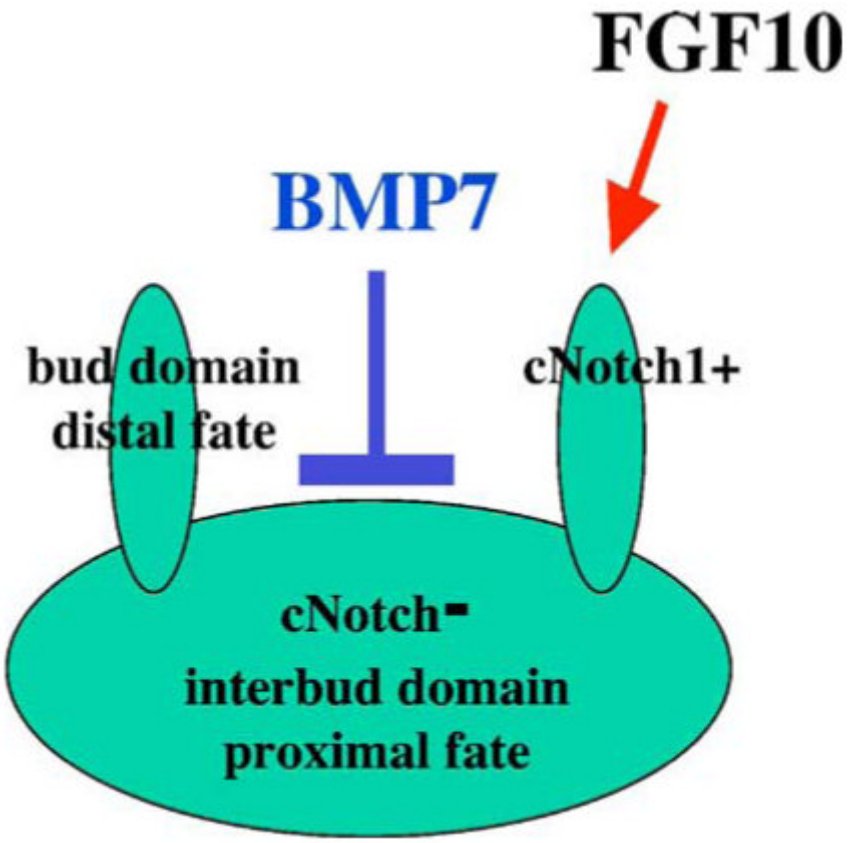

Fig. 6.

Model for branching morphogenesis in the prostate: (1) areas of high Notch1/Hes1 activity are associated with forming prostate buds and with distal tip epithelium; domains of low Notch1 activity are associated with interbud epithelium and may contribute to proximal epithelial fates; (2) BMP7 signaling inhibits formation of the new prostate buds, and limits the number of domains with high Notch1 activity; (3) FGF10 may function to promote extension of the prostate tips by favoring proliferation of the bud epithelium which exhibits high Notch1 activity.